Composites Communications 21 (2020) 100413

Contents lists available at ScienceDirect

Composites Communications

journal homepage: www.elsevier.com/locate/coco

Fused deposition modeling 3D printing of polyamide-based composites and its applications

Xu Zhang [a], Wei Fan [a,*], Tianxi Liu [a,b,**]

[a] Innovation Center for Textile Science and Technology, State Key Laboratory for Modification of Chemical Fibers and Polymer Materials, College of Materials Science and Engineering, Donghua University, Shanghai, 201620, PR China

[b] Key Laboratory of Synthetic and Biological Colloids, Ministry of Education, School of Chemical and Material Engineering, Jiangnan University, Wuxi, 214122, PR China

ARTICLE INFO

Keywords:
Fused deposition modeling
3D printing
Polyamide
Composites

ABSTRACT

Fused deposition modeling (FDM) is one of the most commonly utilized low-cost 3D printing technology, which employs the hot-melt and adhesive properties of thermoplastic materials. As one of the most important classes of engineering thermoplastic polymer materials, polyamide (PA) possesses excellent comprehensive performance. However, the FDM fabricated products based on pure PA are seriously warped, distorted, and lack of shape stability due to the accumulation of shrinkage stress generated from the crystallization of polymer, which severely restrict the application of PA in FDM 3D printing. In this article, notable advances in FDM 3D printing of polyamide-based composites and the properties of the printed parts as well as their practical or potential applications are highlighted. The particular emphasis is placed on the formation and the performance of polyamide/polymer blends, inorganic particle reinforced polyamide composites, and fiber reinforced polyamide composites. Finally, the significant limitations, opportunities, and challenges are identified to motivate the future research on the FDM 3D printing of polyamide-based composites and its applications.

1. Introduction

3D printing (3DP), also known as additive manufacturing (AM), rapid prototyping (RP), and solid-freeform (SFF), is an exponentially evolved manufacturing technology covering a process of joining materials to make objects from 3D model data, usually layer-by-layer, which has received significant attentions in recent years by offering numerous advantages over traditional subtractive methods since it was first described in 1986 by Charles Hull [1]. The 3DP technology provides the ability to directly create objects with intricate geometrical features in a cost-effective way, which requires no mold tool and offers near-net-shape manufacturing in a relatively short period of time [2]. In addition, the 3DP is most beneficial in fabrication of customized parts and products with complex and tailored designs while being capable of harnessing digital information for the realization of a robust and decentralized 3D manufacturing system [3]. Among the various 3DP techniques, fused deposition modeling (FDM) is one of the most commonly utilized low-cost processes due to its simplicity and availability of machines at affordable prices, which employs the hot-melt and adhesive properties of thermoplastic materials [4–7]. During the FDM process, the un-melted filament acts as a piston for pushing the melted polymer out of the nozzle after that the molten filament is deposited onto a platform in a raster pattern in order to form each layer of the model, while the final 3D product is fabricated through building up successive layers (see Fig. 1) [8,9]. Therefore, the materials based on which the filament is fabricated must have adequate stiffness and melt flow-ability [9]. Usually, the thermoplastic polymer-based filaments are used as feedstock materials in FDM, including acrylonitrile butadiene styrene (ABS), polylactic acid (PLA), and polycarbonate (PC), etc. [10].

Despite the wide variety of polymers are available, whereas, the commercial polymeric materials for FDM are still limited, costly, and lack of high properties, which severely hinders the use of FDM technology for manufacturing. Therefore, new filament with low cost and excellent properties for FDM need to be developed urgently. As one of the most important classes of engineering thermoplastic polymers,

* Corresponding author.
** Corresponding author. Innovation Center for Textile Science and Technology, State Key Laboratory for Modification of Chemical Fibers and Polymer Materials, College of Materials Science and Engineering, Donghua University, Shanghai, 201620, PR China.
E-mail addresses: weifan@dhu.edu.cn (W. Fan), txliu@dhu.edu.cn, txliu@jiangnan.edu.cn (T. Liu).

https://doi.org/10.1016/j.coco.2020.100413
Received 15 June 2020; Received in revised form 6 July 2020; Accepted 7 July 2020
Available online 23 July 2020

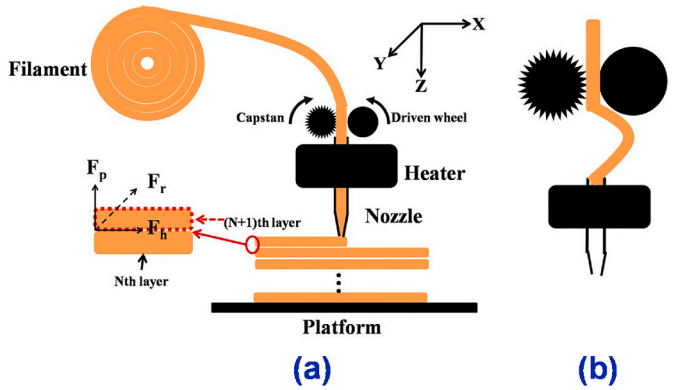

Fig. 1. Schematic diagram of (a) FDM technique and (b) breakdown caused by the buckling of filament. Reprinted with permission from Ref. [8].

polyamide (PA or nylon) possesses excellent comprehensive performance. Unfortunately, a large number of attempts indicated that the FDM fabricated products based on pure PA are seriously warped, distorted, and lack of shape stability. Such drawbacks severely restrict the application of PA in FDM 3D printing. The reason why for severe warpage of 3D printed PA is ascribed to the accumulation of shrinkage stress generated from the crystallization of polymers. The successive stacking of crystalline polymers leads to asynchronous volumetric shrinkage, and the regular arrangement of molecular chains critically aggravates the shrinkage and warpage. Therefore, the critical factor to prevent the warpage in FDM is to hinder the regular arrangement of molecular chains and weaken its ability to crystallize [8,11]. In the FDM process, the filament melt into a liquid or semi-liquid state at nozzle and then was extruded layer-by-layer onto the former deposited layer or build platform, where the layers are fused together and then solidify into final parts. To some extent, the quality of FDM 3D printed parts can be tailored by altering printing parameters, such as layer thickness, printing orientation, raster width, raster angle, and air gap, which have been discussed by Sood et al. [12]. By contrast with processing parameters, the development of new FDM 3D-printable material or filament is of

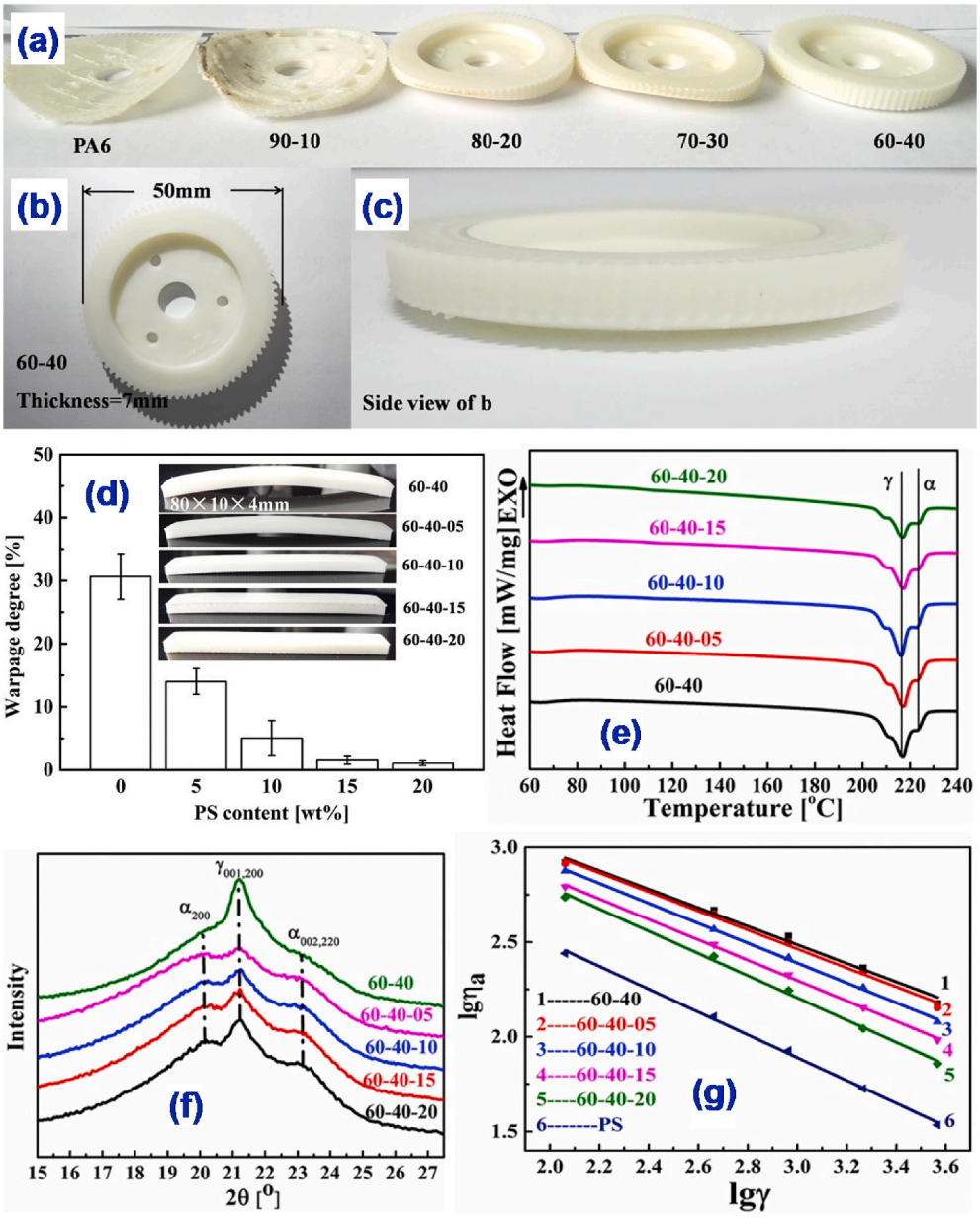

Fig. 2. (a) The printed samples based on a gear model using different PA6/POE-g-MAH composites, (b) planform of 60-40-based printing product, (c) side view of the 60-40-based printing product, (d) the warpage degree of the 3DP products based on 60-40/PS composites, (e) melting curves of 60-40/PS composites, (f) XRD patterns of 60-40/PS composites, and (g) rheological property of 60-40/PS composites. The multi-number label (two-number N-M or three-number N-M-L) represents the mass ratio of PA6, POE-g-MAH, and PS in the composites from left to right. Reprinted with permission from Ref. [8].

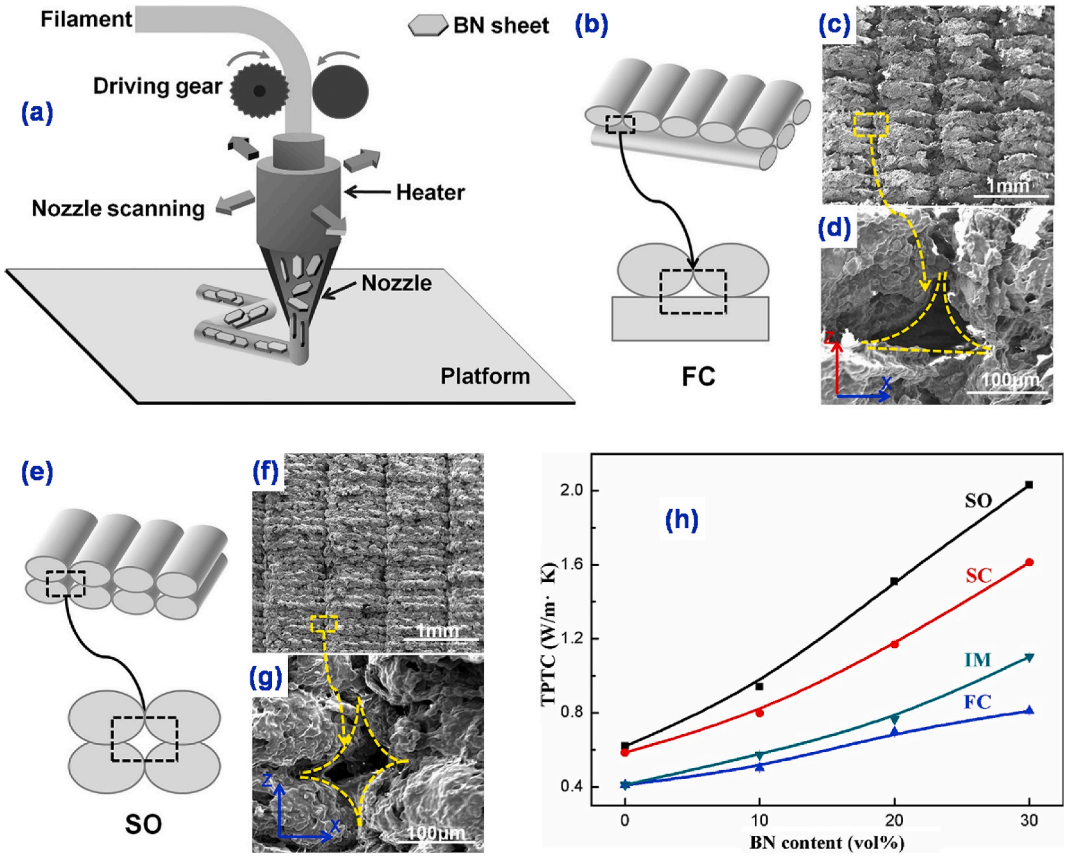

Fig. 3. (a) Schematic diagram of FDM technology and the h-BN sheets orientation during the process of fused deposition. Schematic diagrams of formation mechanism of the voids in different printing methods (b) flat-cross (FC) printing and (e) stand-in-order (SO). Morphology of voids inside the samples (c, d) FC with 30 vol% h-BN and (f, g) SO with 30 vol% h-BN. (h) TPTCs of stand-in-order (SO) printing, stand-cross (SC) printing, injection moulding (IM), and flat-cross (FC) printing samples. Reprinted with permission from Ref. [17].

much more crucial of importance in determining the properties of the final fabricated products.

With the high demands for practical applications, the polymer matrix composites have become state-of-the-art in material design and development for 3D printing, which could improve the properties of polymers by combining the matrix and reinforcements to achieve a composite system with more useful structural or functional properties non attainable by any of the constituent alone [10,13–15]. In recent several years, the sophisticated development of polymer composite materials that are compatible with the available 3D printers has certainly created more opportunities for PA in FDM applications, especially in the development of advanced and multifunctional PA-based composites. Also, there has been considerable achievements in developing new FDM 3D printable polyamide-based composites with improved performance. Hence, in this review, we present, analyze, and summarize the advanced progress in FDM 3D printing of polyamide-based composites and its applications. Based on the type of reinforcement, the main part of this review article is organized into three sections including polyamide/polymer blends, inorganic particle reinforced polyamide composites, and fiber reinforced polyamide composites. In the final section, we make an attempt to point some future directions for the further development of FDM 3D printing of polyamide-based composites and its applications.

2. Polyamide/polymer blends

In a few recent studies, the crystalline polyamide 6 (PA6) were modified by introducing amorphous polymer to prevent the severe warpage so that it could be applied to FDM technology. Jia and He et al. [8] have developed a new kind of PA6-based filament with good toughness for FDM via a facile method, in which the maleic anhydride grafted poly(ethylene 1-octene) (POE-g-MAH) was introduced into PA6, forming PA6/POE-g-MAH blend, to disturb the crystallization and reduce the shrinkage stress. The amorphous POE-g-MAH has numerous short-chain branches and good compatibility with PA6 which could effectively impede the regular arrangement of PA6 molecular chains during cooling process, resulting in lower shrinkage and reduced stress which induces the warpage. Simultaneously, the amorphous POE-g-MAH also acts as parts of the polymer matrix which is used in FDM process. It can be observed from Fig. 2a–c that the warpage of FDM printed gears could be reduced as the content of POE-g-MAH increases. To further decrease the warpage, the amorphous polystyrene (PS) with rigid chain segments was introduced into the PA6/POE-g-MAH binary blend system to further improve the shape stability of FDM products. In this PA6/POE-g-MAH/PS ternary blend system, the POE-g-MAH and PS both acts as amorphous phase and warpage modifier in the blend, which will reduce the shrinkage stress and promote the shape stability of the FDM 3D printed products. Besides, the POE-g-MAH acting as compatibilizer will give good compatibility between PA6 and PS. It was observed that the warpage degree of the FDM 3D printed products based on PA6/POE-g-MAH/PS ternary blend decreases as the loading of PS increases, which reduces to only 1.06% with the PS loading of 20 wt% (see Fig. 2d). The DSC (Fig. 2e), XRD (Fig. 2f), and rheological (Fig. 2g) results revealed that the amorphous PS would reduce the uniformity of molecular chains in the ternary blend leading to a decrease in the crystallinity of PA6. Moreover, the FDM 3D printed products based on PA6/POE-g-MAH/PS exhibit good mechanical properties, where the tensile, flexural, and impact strength attains 24.1 ± 0.7 MPa, 31.5 ± 1.3 MPa, and 33.5 ± 1.2 kJ/m^2, respectively.

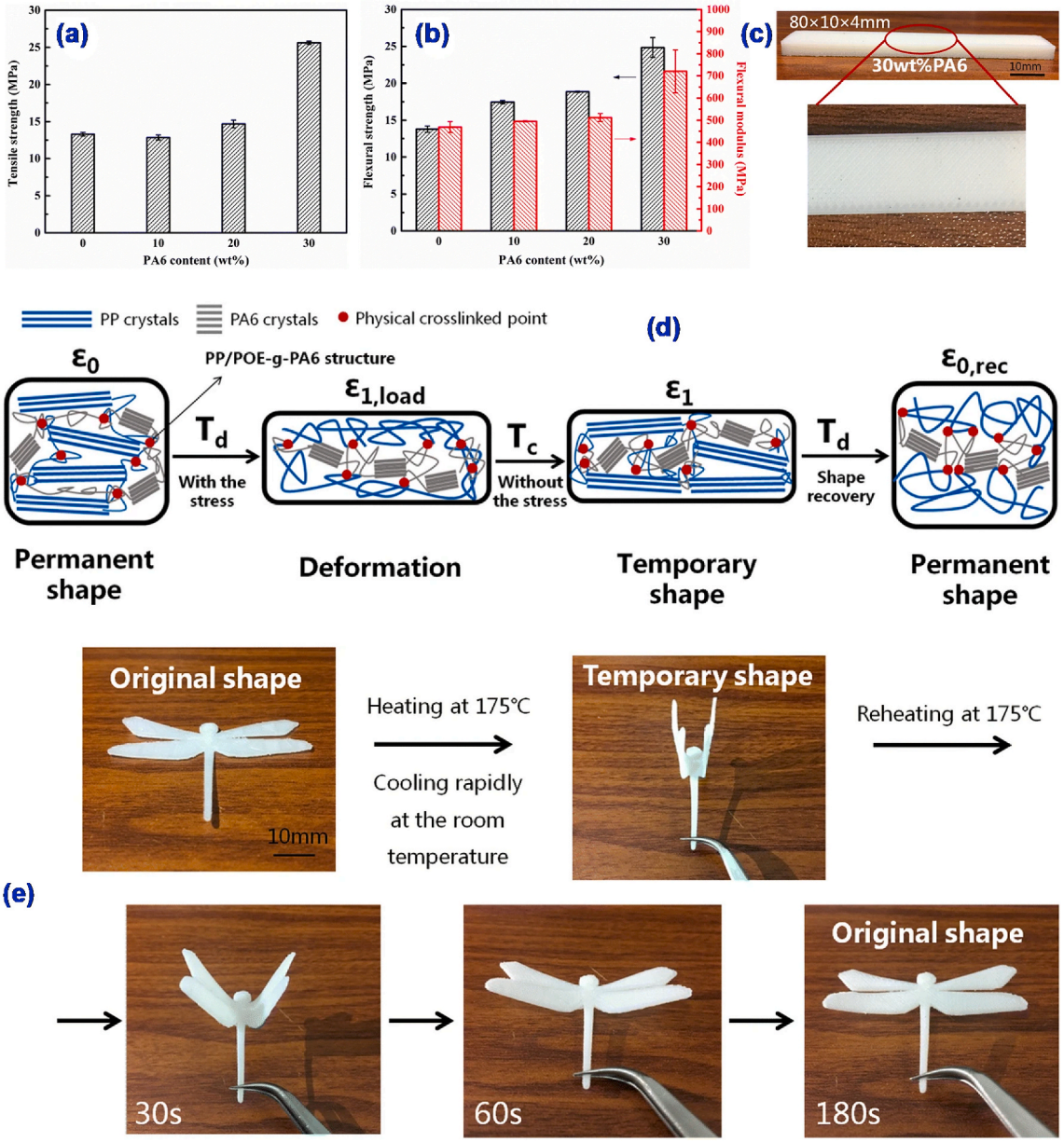

Fig. 4. (a) Tensile and (b) flexural properties of 3D printed products based on PA6/POE-g-MAH/PP alloys with different PA6 contents. (c) The printed product quality based on 30 wt% of PA6 in the PA6/POE-g-MAH/PP blends. (d) Schematic diagram of shape memory effect (SME) based on PA6/POE-g-MAH/PP alloys. (e) Photographs showing the SME of the 3D printed product based on PA6/POE-g-MAH/PP alloy with 30 wt% of PA6. The mass ratio of PP and POE-g-MAH is fixed at 1.5:1. Reprinted with permission from Ref. [11].

Based on the success in FDM 3D printing of PA6/POE-g-MAH binary and PA6/POE-g-MAH/PS ternary blend, the high through-plane thermal conductivity (TPTC) composites with high thermally conductive reinforcements (such as graphite and boron nitride) were further achieved via FDM. In virtue of the characteristics and great design flexibility of FDM, the special design of FDM 3D printing process can make the anisotropic thermally conductive filler orient along the through-plane direction or align vertically, which would obviously improve the TPTC of the FDM-printed products. Firstly, in 2017, Jia and He et al. [16] chose the anisotropic flake graphite, which is naturally abundant and low-cost, as the thermally conductive modifier for PA6/POE-g-MAH/PS blend with a mass ratio of 12/8/5 to fabricate high TPTC products. The orientation of graphite flakes and the distribution of voids in FDM fabricated products, which are key points for TPTC, are significantly affected by the printing strategy. The optimal PA6/POE-g-MAH/PS/graphite products show a high TPTC as 5.5 W m^{-1} K^{-1}. Meanwhile, a heat sink with good thermally conductive property used for the FDM 3D printer was successfully fabricated and it can well meet the heat dissipation requirement of FDM 3D printer. Then in 2019, Geng and He et al. [17] adopted the previously as-prepared PA6/POE-g-MAH with a mass ration of 60/40 as the polymer matrix and anisotropic hexagonal boron nitride (h-BN) as the thermally conductive filler to fabricate the TPTC composites via FDM (Fig. 3a). In this study, three FDM 3D printing methods have been designed to regulate the orientation of h-BN sheets (Fig. 3a), which declares that the suitable design can reduce the negative effects of voids produced during the deposition of filaments (Fig. 3b–g). The enhanced TPTC of PA6/POE-g-MAH/h-BN composites with vertical alignment of h-BN were achieved, and the maximum TPTC reaches 2.03 W m^{-1} K^{-1} (Fig. 3h). It was proved that the FDM is an effective method to fabricate high TPTC products using less fillers by reasonable design. Therefore, the as-prepared new kind of POE-g-MAH as well as POE-g-MAH/PS

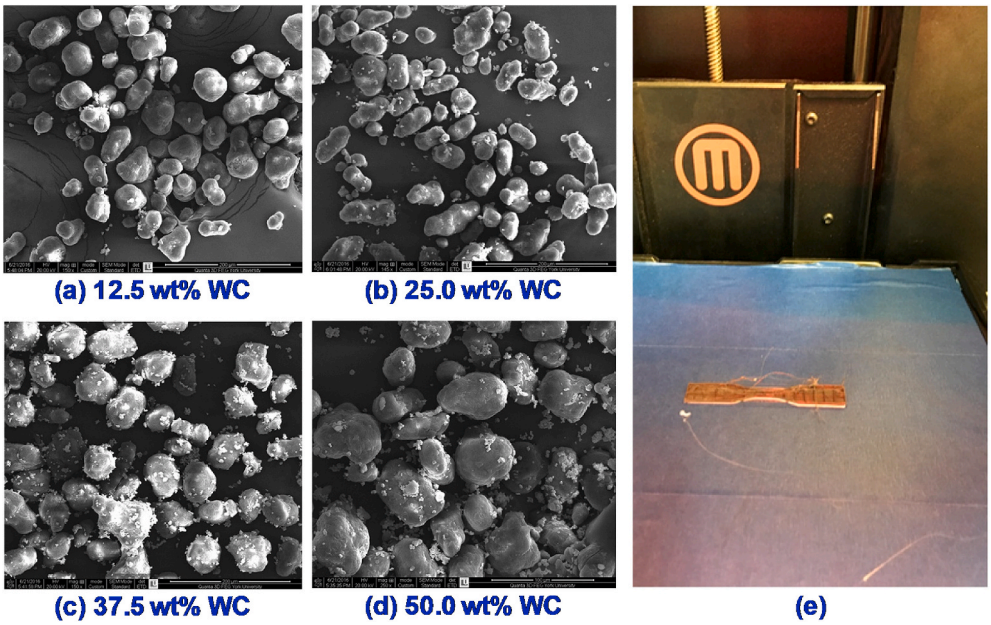

Fig. 5. (a–d) SEM Images of various powder mixtures (scale bar = 100 μm). (e) Fabrication of tensile test part by FDM. Reprinted with permission from Ref. [20].

modified PA6 filaments with good 3DP (FDM) performance may open new opportunities for solving the printing problem encountered in PA6 for FDM 3D printing.

Since the four-dimensional (4D) printing concept was first proposed in 2013, it has aroused widespread interests among society and academy, which has introduced the fourth dimension of "time" on the basis of 3D printing, whereas the 3D printed products are capable of varying in structure, shape or function over time [11,18,19]. Recently, Peng and He et al. [11] designed a novel filament with shape memory performance based on PA6/polypropylene (PP) blend for FDM, in which the maleic anhydride-grafted poly(ethylene-octene) (POE-g-MAH) was also used as a modifying agent as well as a compatibilizer. A high dimensional stability and appropriate mechanical properties of FDM printed parts based on PA6/POE-g-MAH/PP alloy were obtained at 30 wt% PA6 loading with the certain mass ratio of PP and POE-g-MAH of 1.5:1 (Fig. 4a–c). In addition, the possibility of PA6/POE-g-MAH/PP as a shape memory polymer blend and the mechanism of shape memory effect (SME) were investigated (Fig. 4d). The FDM 3D printed products with 30 wt% of PA6 fabricated by the infill orientation of 45°/-45° and 100% infill density exhibited a great SME with the deformation temperature (T_d) of 175 °C (Fig. 4e). In this study, the use of the semi-crystalline polymer blend based on PA6/POE-g-MAH/PP alloy in FDM can produce complex and smart parts that exhibit heat-activated shape memory performance in a simple way. Moreover, it is also beneficial to promote the development of 4D printing technology and applications in advanced fields.

In addition to the amorphous polyolefin (POE-g-MAH, PS, and PP) reinforced PA6 composite filaments, Farina and Fraternali et al. [29] developed a new kind of PA6-based filaments for FDM, which couples high mechanical properties with eco-sustainability. The high-performance PA6 sustainable filaments were extruded from recycled PA6 granulates through a dedicated twin-screw extrusion line, which processes either pure recycled PA6 grains, or mixtures of such a material with a minor amount of acrylonitrile butadiene styrene (ABS) and titanium dioxide (TiO_2), denoted by PA6/ABS and PA6/TiO_2, respectively. Such kind of PA-based filament performed very well in dimensional stability, as no warping or curling issues were observed during FDM printing process. In terms of mechanical performances, the mixture of PA6/ABS is particularly adaptive with the highest tensile strength and Young's modulus among the examined recycled PA6-based materials. Overall, it can be concluded that the PA6 granules/filaments have shown great eco-sustainability, excellent mechanical strength, and stable thermal properties after recycling, which makes them feasible to use for various 3D printing applications.

3. Inorganic particle reinforced polyamide composites

Inorganic particle reinforcements are widely used to improve the properties of polymer matrix thanks to their low cost and ease of mixing, which permits the fabrication of inorganic particle reinforced polymer (IPRP) composites. The IPRP composites with reinforcements in forms of metallic, ceramic, carbon particles exhibit high mechanical performance and excellent functionality, which could be extruded into printable filaments for FDM process. The advanced progress in the FDM 3D printing of IPRP composites, including improved tensile and storage modulus by adding iron (Fe) or copper (Cu) particles [21], improved wear resistance by adding aluminum (Al) and aluminum oxide (Al_2O_3) [22], and improved dielectric permittivity by adding ceramic [23] or tungsten [24] particles, makes it possible to fabricate IPRP composite products with high performance as well as multi-functionality for the potential real-world applications in a variety of fields. Importantly, the addition of inorganic particles into polyamide matrix helps to enhance the shape or dimensional stability of FDM 3D printed products based on polyamide composites.

3.1. *Metallic particle reinforced polyamide composites*

Embedding metallic particles, including metallic compounds and metal powders, into polyamides was proved to be an efficient solution to improve the properties of final FDM printed parts. When combining with metallic particles, the polyamide composites showed a large reduction in coefficient of thermal expansion, thus the distortion or warpage of FDM printed specimen remarkably reduced. Based on the special thermal properties of metallic compounds, Kumar and Czekanski [25] undertook an investigation to utilize waste PA powders produced by selective laser sintering (SLS), an additive manufacturing (AM) process, to make low-cost metallic compounds reinforced PA composite filaments. Firstly, the discarded SLS polyamide 12 (PA12) powders were mixed with various weight percentages (12.5, 25, 37.5, and 50 wt%, see Fig. 5a–d) of tungsten carbide (WC) to enhance the mechanical and

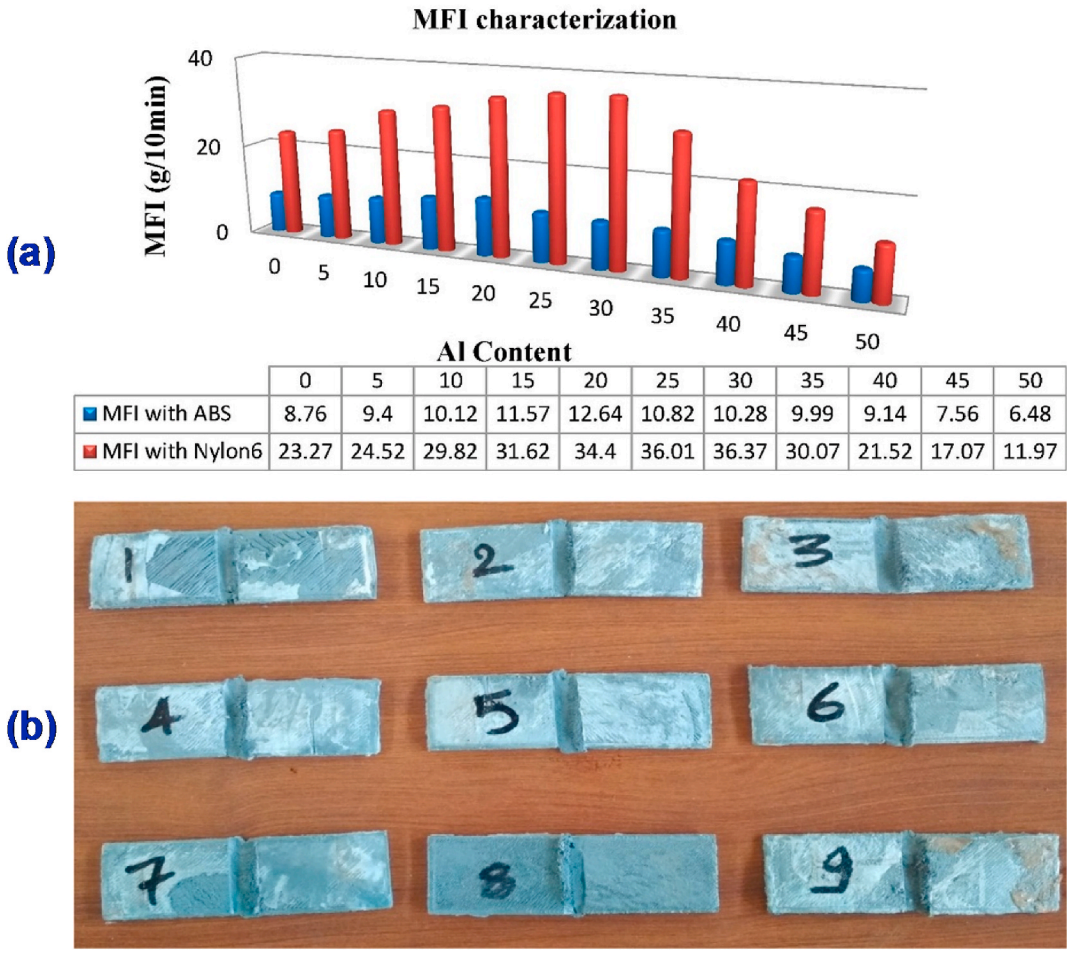

	0	5	10	15	20	25	30	35	40	45	50
MFI with ABS	8.76	9.4	10.12	11.57	12.64	10.82	10.28	9.99	9.14	7.56	6.48
MFI with Nylon6	23.27	24.52	29.82	31.62	34.4	36.01	36.37	30.07	21.52	17.07	11.97

Fig. 6. (a) Variations in MFI of ABS and PA6 over Al proportions. (b) Welded parts with various input process parameters. Reprinted with permission from Ref. [29].

dimensional properties. Then, the differential scanning calorimetry (DSC) and melt flow index (MFI) tests were performed to determine the suitability of powder mixtures for FDM. Finally, a single screw extruder was used to process these PA12/WC powder mixtures to form WC reinforced PA12 (PA12/WC) composite filaments for testing. It was found that the addition of WC has increased glass transition temperature, MFI, and the strength of resulting PA12/WC composites. Moreover, the as-prepared PA12/WC composites possess adequate mechanical property (tensile strength, Young's modulus, elongation at break from 25 to 60 MPa, 700–1300 MPa, 260–700%, respectively) and is compatible with FDM machine, which can be used to successfully build 3D structures from an FDM system (Fig. 5e). In another recent work, Soundararajan et al. [26] took an insight examination for successfully fabrication of titanium dioxide (TiO_2) reinforced PA6 (PA6/TiO_2) composites for FDM 3D printing. The appraisal outcome of FDM-fabricated samples indicated that the incorporation of TiO_2 could markedly influence the mechanical and tribological (wear rate) properties of pure PA6, where the tensile strength and Young's modulus increases while the elongation at break and wear rate decreases with increase of TiO_2. The examined experiment revealed that the PA6/TiO_2 composites had better FDM 3D printing property, mechanical strength, and wear resistance than the pure PA6.

The metal powders are another promising additive to promote the FDM 3D printing properties of polyamide matrix. In this respect, Kumar and Singh et al. [27–32] have made great contributions to developing the 3D printable metal powder reinforced PA6 composites to fabricate functional and non-functional prototypes using the FDM process for friction welding or solid-state welding applications. The composite feedstock filament composed of ABS and PA6 with reinforcement of

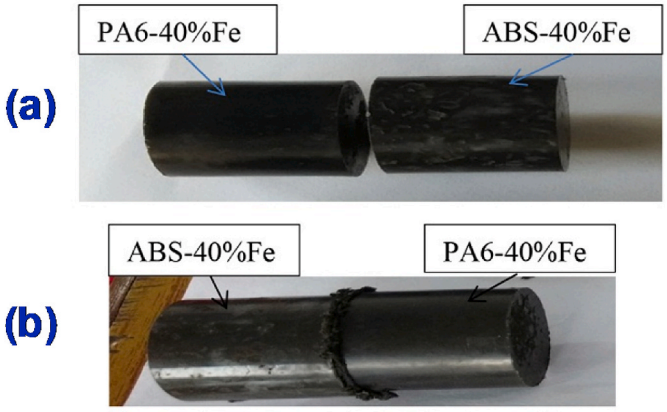

Fig. 7. (a) FDM fabricated parts of ABS-40%Fe and PA6-40%Fe. (b) Frictionally welded parts. Reprinted with permission from Ref. [29].

aluminum (Al) powder has been successfully developed for FDM 3D printing of prototype in friction welding applications [27–31]. The results of these studies suggested that the addition of Al reinforcement at a certain level to ABS and PA6 matrix resulted in the similar range of MFI (Fig. 6a), melt point as well as specific heat capacity of these two different thermoplastic polymers, ensuring that the ABS/Al and PA6/Al composites are feasible and mechanically compatible for friction welding. After preparation of feedstock filaments of selected ABS/Al and PA6/Al composites, the welded components with low warpage were

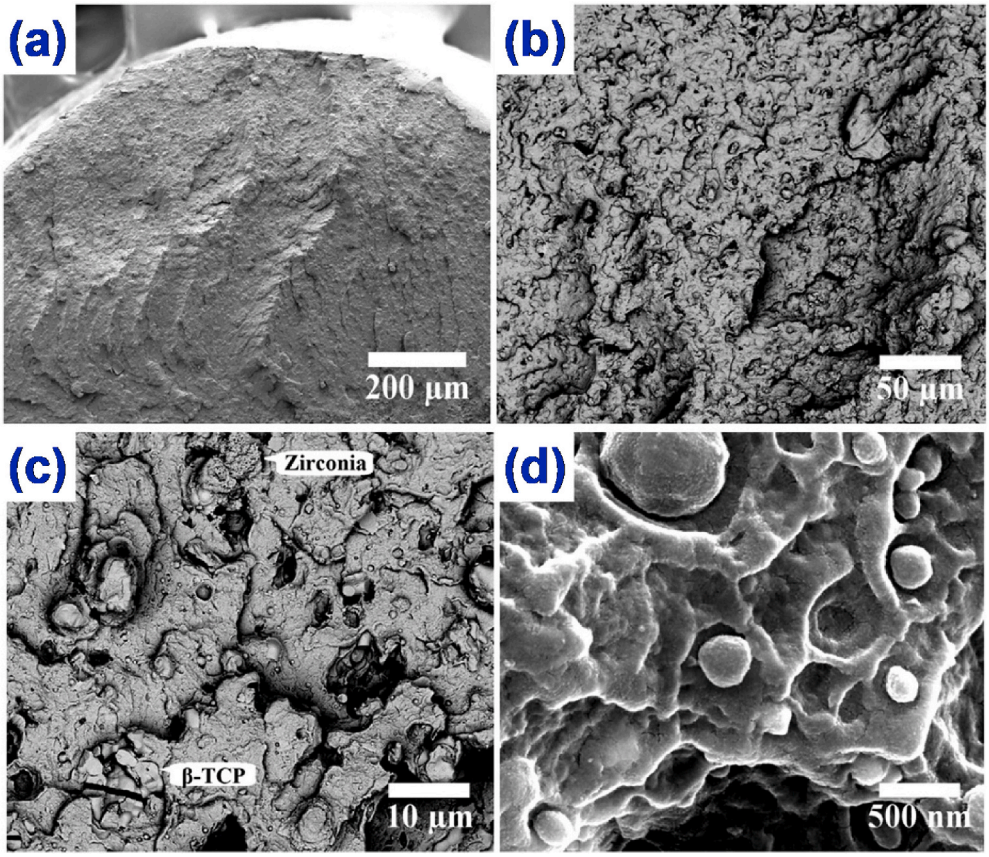

Fig. 8. Microstructure of 40% hybrid filled PA12 filament feedstocks at (a) 300×, (b) 1000×, (c) 5000×, and (d) 100,000× magnification. Reprinted with permission from Ref. [35].

fabricated by FDM 3D printing for friction welding applications (Fig. 6b). Furthermore, it has been observed that the high mechanical strength was achieved by minimizing porosity in feedstock filament and the FDM 3D printed structural components of selected thermoplastic composites were gainfully friction welded. In 2018, Kumar and Singh et al. [32] have done a further research on iron (Fe) powder reinforced PA6 matrix and ABS matrix, respectively, for friction welding. Two functional prototypes of circular cross-section were prepared on FDM machine with PA/Fe and ABS/Fe composite filament, respectively. Under best parametric conditions of feed, rotation speed, etc. these Fe powder reinforced PA6 and ABS were successfully joined (see Fig. 7).

3.2. Ceramic particle reinforced polyamide composites

Up to date, the ceramic materials, a very important class of inorganic particles in composites, have been successfully employed in polymer matrix composites, due to their extremely high thermal, mechanical, as well as biological properties. Therefore, ceramic materials have also been used as reinforcements for the 3D printing of polyamide-based composites. Recently, Rahim et al. [33] developed a new composite consisting of polyamide 12 (PA12) incorporated with zirconia (ZrO_2) and hydroxyapatite (HAP) particles using the FDM 3D printing technique. At the expense of reduced toughness and flexibility, the incorporation of ceramic fillers improved or maintained the strength, stiffness, and thermal stability of neat PA12. Meanwhile, a slight decrease in the degree of crystallinity was also observed as a result of loading ceramic filled particles. In summary, the PA12/ceramic (PA12/ZrO_2/HAP) composites were found to perform well with FDM technique and enabling the production of medical implants with acceptable mechanical performances for non-load bearing applications. Almost during the same period, Abdullah et al. [34,35] achieved the hybrid bio-ceramic filled PA12 composite feedstock filament (see Fig. 8) for craniofacial reconstruction via FDM framework, where the fixed 15 wt% loading of zirconia (ZrO_2) as well as various weight fractions (30 wt %, 35 wt%, 40 wt%, etc.) of beta-tricalcium phosphate(β-TCP) were compounded with PA12 to tailor the printability of the PA12 composites. According to assessment on the melt flow rate (8–9.5 g/10 min), mechanical properties (8%–31% and 98%–181% increase in tensile modulus and impact strength, respectively), and physical or cytotoxicity properties (high surface roughness or significant increase in the viability of human periodontal ligament fibroblast cells), it indicated that the hybrid ceramics filled PA12 (PA12/ZrO_2/β-TCP) composites with improved properties is sufficiently suitable for an FDM-based 3D printer, which enables the creation of patient-specific craniofacial implant at a lower cost to serve low-income patients. These studies on ceramic particles reinforced polyamide composites are essential for the success of future research.

3.3. Carbon particle reinforced polyamide composites

Carbon particles, including graphene, carbon nanotube (CNT), graphite, and carbon black (CB), often exhibit unique mechanical, electrical, and thermal properties, which could enable the fabrication of high-performance functional composites through the addition into polymers for 3D printing. Graphene, due to its outstanding properties, has become the topic of much research activities and is assumed to be potential reinforcing fillers for polymer-based composites. In 2016, Xi et al. [36] have investigated the possibility of graphene reinforced polyamide 6 (PA6/graphene) composites for FDM 3D printing technology, where the PA6/graphene composite materials were prepared by melt blending method and the FDM process of the materials were examined by orthogonal test. An optimized processing condition was

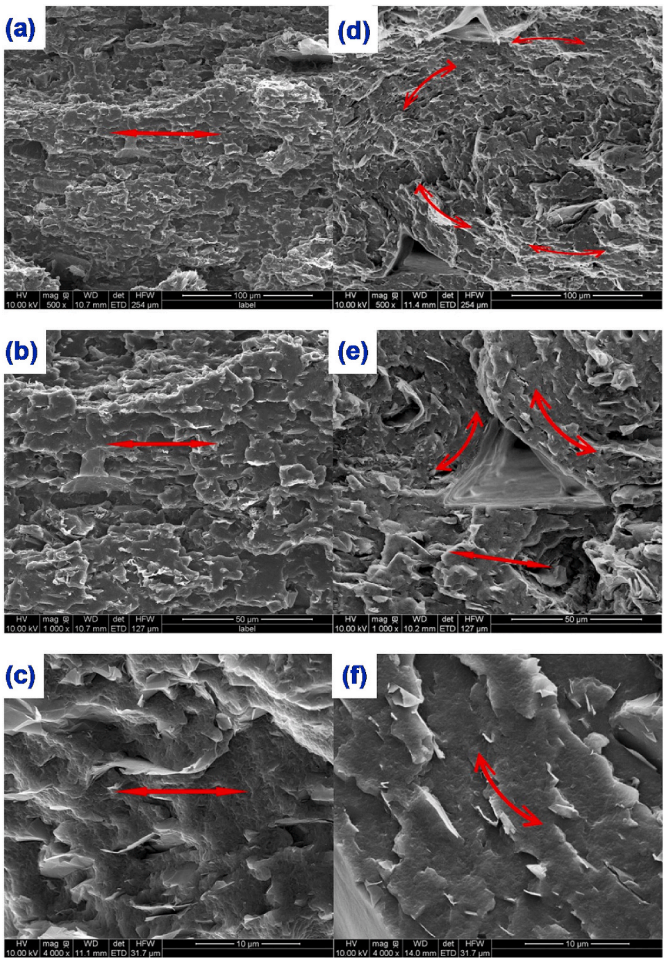

Fig. 9. SEM images showing the fracture surface of 3D printed (a–c) 90°and (d–f) 0° PA12 filled with 6 wt% graphene nanocomposite specimens. Reprinted with permission from Ref. [37].

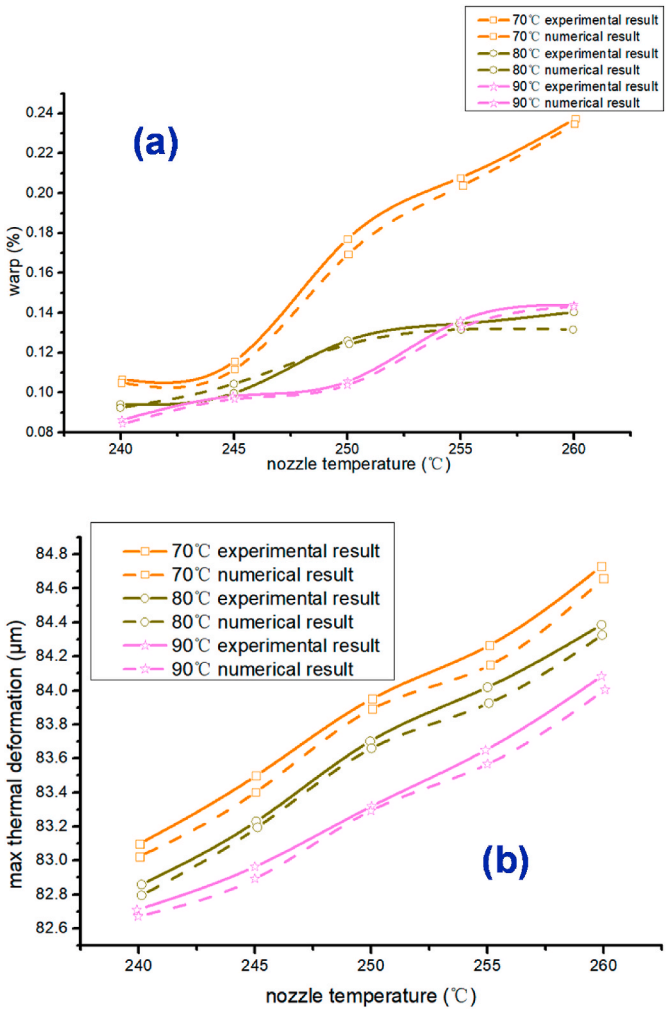

Fig. 10. Numerical and experiment (a) workpiece warpage at different hot-bed temperatures and (b) maximal workpiece thermal-deformation displacement at different hot-bed temperatures. Reprinted with permission from Ref. [38].

obtained for the PA6/graphene composite materials in FDM, when the nozzle temperature is 245 °C, the platform temperature is between 60 °C and 70 °C, the printing speed is 27 mm/s, the nozzle diameter is 0.4 mm, and the slice thickness is 0.20 mm. For the mechanical properties of the product, the order of the influence factor is as follows: the content of the graphene, the temperature of the nozzle, the printing speed and the platform temperature. When the mass fraction of graphene is 0.05%, the forming parts printed on the basis of the technological parameters in FDM can yield the best mechanical properties. In the following year (i.e. 2017), Zhu et al. [37] prepared printable polyamide 12 (PA12) nanocomposite filaments with 6 wt% graphene nanoplatelets for FDM and smoothly printed via a commercial FDM 3D printer. The thermal conductivity and elastic modulus along the printing direction of 3D printed PA12/graphene specimen increased by 51.4% and 7% than that of compression molded counterparts with the ultimate tensile strength well maintained simultaneously. Moreover, it can be explained by both tensile and DMA test that the raster angle of 0° printed PA12/graphene parts exhibit the best reinforcement efficiency due to the orientation behavior of graphene nanoplatelets in PA12 matrix (see Fig. 9). These results indicated that FDM is a new way to achieve PA12/graphene composites with enhanced thermal conductivity over compression moulding, which could contribute to efficient and flexible heat management for a wide range of applications.

Polyamide 66 (PA66) is a material with high wear resistance, toughness, and heat resistance. However, low stiffness and thermal deformation during thermal processes restrict its applications in many conditions. Recently, Li and Sun et al. [38] produced filaments of PA66 reinforced with carbon powder (CP, particles with 0.01 ± 0.005 mm) for FDM 3D printing, where the influence of FDM processing parameters on the thermal-deformation degree of composite material was thoroughly examined. It was verified that adding carbon powder is helpful in enhancing the stiffness and reducing the thermal deformation. In terms of warpage or dimensional stability, the average warp of pure PA66-forming workpiece was 0.1953% and the average warpage of PA66 with 20% carbon powder (PA66/CP-20%) composite was 0.0982%, indicating that the warpage of the FDM 3D printed workpiece decreases by 49.7% after adding 20% carbon powder. Besides, after adding carbon powder into PA66 matrix, the maximal thermal deformation displacement of the specimen was reduced by 11.4% (from 90.46 μm to 80.167 μm). Based on comparing experiments and simulations (see Fig. 10), it was found that 20% carbon mass fraction was best for the comprehensive performance including the maximal thermal-deformation displacement and warp of the forming workpieces when the nozzle and hot bed temperature was 240 °C and 90 °C, respectively.

4. Fiber reinforced polyamide composites

Fibers including glass fibers (GF) and carbon fibers (CF), etc., are commonly used reinforcements to improve the mechanical properties of polymer matrix materials. FDM is one of the widespread 3D printing

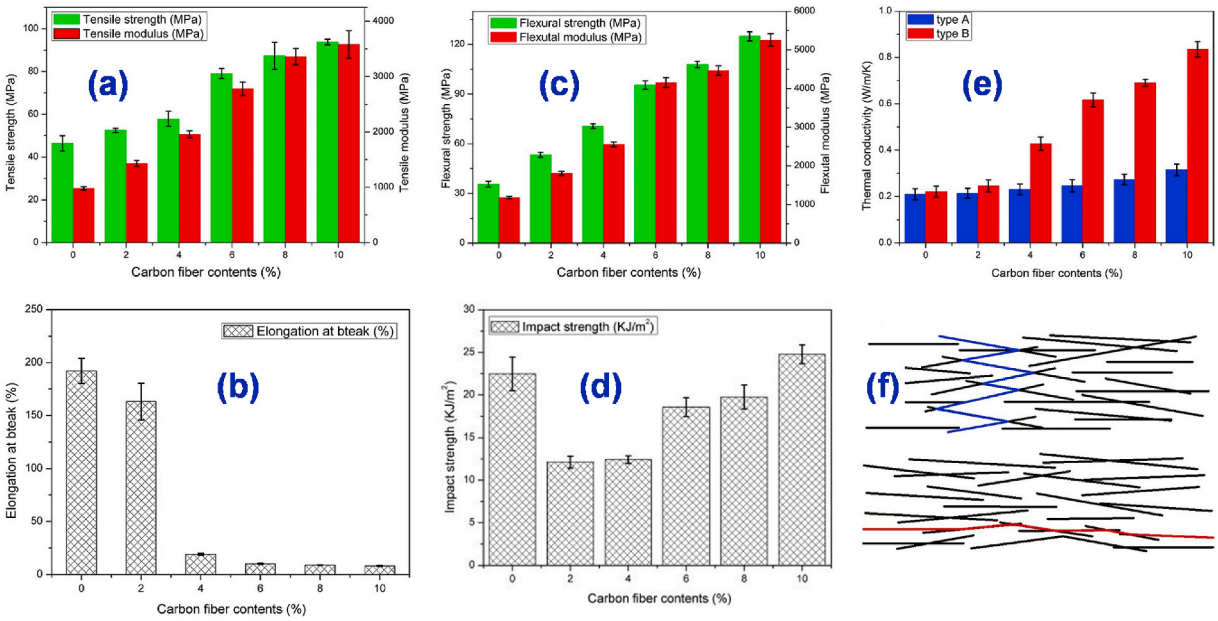

Fig. 11. (a) Tensile strength and tensile modulus, (b) elongation at break, (c) flexure strength, (d) Impact strength, and (e) thermal conductivity of pure PA12 and carbon fiber reinforced PA12 composites with 2, 4, 6, 8, and 10 wt% carbon fiber. (f) Schematic illustration of heat-channel in the matrix of two types. Reprinted with permission from Ref. [39].

technology to produce fiber reinforced polymer composites. For the FDM process, the polymer pellets and fibers are usually mixed in a blender first and then delivered to extruder to form filaments. Note that a second extrusion processing could be implemented to make sure the homogenous distribution of fibers in the polymer matrix. In the fiber reinforced polymer composites, the fiber orientation and void fraction of composites plays an important role in determining the final properties of the composites. However, in practical FDM technology, each layer is formed through the deposition of a filament and the direction or arrangement of the filament deposition (and therefore of the reinforcement, if present) changes during the formation of the contour and the infill. Therefore, the fibers can be oriented differently inside the

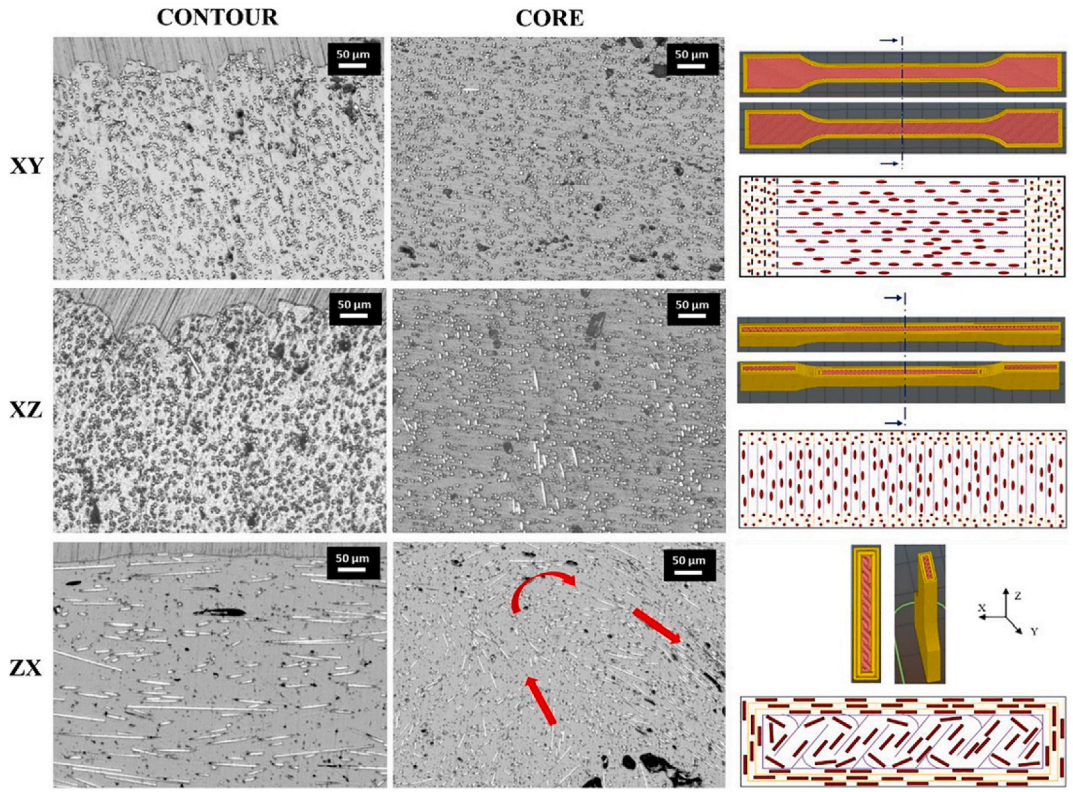

Fig. 12. Orientation of fibers inside the tensile samples observed on the cross section of samples processed according to different orientations and schematic representation of expected specimen microstructures. Red arrows show as the fiber orientation changes as a function of the variation of the filament deposition direction. Reprinted with permission from Ref. [40].

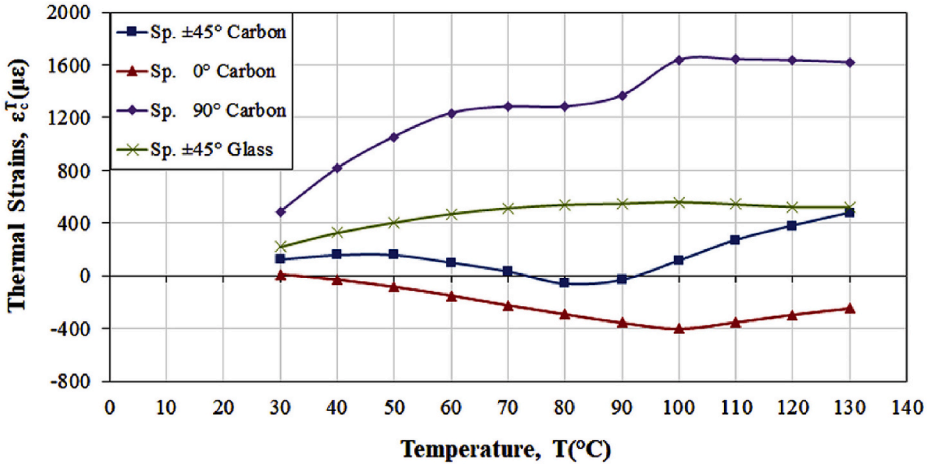

Fig. 13. Thermal strains as a function of applied temperature for all FDM-fabricated composite samples. Reprinted with permission from Ref. [41].

printed parts depending on the positioning of the component on the building platform, which could provide an isotropic mechanical behavior for the FDM-fabricated polymer/fiber composite products.

Liao et al. [39] reported the thermal and mechanical properties of carbon fiber (CF) reinforced polyamide 12 (PA12) composites by FDM 3D printing (see Fig. 11), where the continuous carbon fibers were cut into about 15–20 mm in length. The printable filaments of PA12/CF composites with different mass fraction for FDM were fabricated by melting compounding using a co-rotating twin screw extruder and the carbon fibers were dispersed homogenously in PA12 matrix. It was found that the crystallization peak temperature and the degradation temperature increased 3.46 °C and 7.50 °C respectively after adding 10 wt% carbon fibers. Compared with the pure PA12 parts fabricated by FDM, the addition of 10 wt% carbon fibers into the PA12 matrix can bring about an observable increase in tensile strength (102.2%), modulus values, and flexural strength (251.1%) without sacrificing the impact property (see Fig. 11a–d). Owing to the establishment of heat-channel, the thermal conductivity along the printing direction increased 277.8% compared with the pure PA12, from 0.221 W m^{-1} K^{-1} to 0.835 W m^{-1} K^{-1} (see Fig. 11e and f). The excellent properties of the parts fabricated by FDM can be explanted by the dispersibility and the extrusion inducing preferential orientation of carbon fiber in the PA12matrix. This work can provide a kind of composite with excellent properties and further expand the application for FDM.

Badini et al. [40] investigated the effect of fiber orientation on the mechanical properties of chopped carbon fiber (sCF) reinforced polyamide 6 composites processed by FDM 3D printing, where the tensile samples with different fiber orientations and layer interfaces with respect to the sample axis (and therefore to the tensile load) were produced (see Fig. 12). It was found that the best strength and stiffness were observed when the fibers and the layer interfaces were parallel to the sample axis, while these properties were about 60% lower when measured in the direction perpendicular to the fibers. The orientation of fibers, occurring to a greater degree in the FDM process, exerted a major influence on the mechanical behavior, exceeding the effects produced by the matrix characteristics (kind of polyamide matrix, matrix crystallinity, and porosity degree) or by the fiber length and percentage. Furthermore, the placement of the layer interfaces (which depends on part orientation) affected the mechanical behavior because the fracture mechanism involved debonding between the stacked layers when the interfaces were placed perpendicular to the loading direction. For these reasons, the orientation of a composite component with respect to the building platform should be carefully considered when designing an additive manufacturing process, in order to grant a favorable orientation of the fibers in the directions where better mechanical properties are required.

In the last few years, the most investigations on FDM 3D printing of fiber reinforced polymer (FRP) composites have been focused on short fiber reinforced polymer composites. Even though such composites attain enhanced mechanical, electrical, and thermal properties compared to conventional FDM-fabricated pure polymeric parts, their performance is still inferior to that of conventionally manufactured FRP composites, which are mainly reinforced by continuous fibers. Therefore, the employment of continuous reinforcing fibers in FDM, such as carbon, aramid or glass, has attracted increasing research attentions. Kousiatza et al. [41] demonstrated the applicability of optical fiber Bragg grating (FBG) sensors for in-situ characterization of continuous carbon and glass fiber reinforced nylon (polyamide, PA) composites fabricated through the FDM technique to investigate in real-time the residual strains and the temperature profiles generated during the fabrication process. The prismatic carbon and glass fiber reinforced nylon (polyamide) composite specimens were built with various fiber orientations through a MarkTwo desktop 3D printer and the FBGs were embedded along with thermocouples into the middle-plane of the composite structures for simultaneous monitoring of both residual strains and temperature profiles developed during the building procedure. The experimental results revealed that the fiber type and orientation strongly impact the process generated temperature profiles and residual strains, as well as the coefficients of thermal expansion of the composite specimens. The marked changes in the obtained slopes of the thermal strains-temperature graph (see Fig. 13) were exhibited when the applied temperature, throughout the heating cycle, exceeds the glass transition temperature (T_g) of the composite samples and in the temperature range from 80 °C to 100 °C. Furthermore, the conducted experiments clearly demonstrated the ability of FBG sensors to accurately determine the in- and post-process induced residual strains, as well as the thermal expansion behavior of FDM-fabricated continuous fiber reinforced thermoplastic composites. It can be convinced from this study that the fiber reinforcement within the 3D printed composite samples significantly reduces the fabrication generated residual strains.

Due to the excellent specific strength and stiffness of continuous fibers, the production of continuous carbon fiber composites using FDM could address the problem of low mechanical properties of raw- or short-fiber reinforced polymer composite parts. He et al. [42] quantified the adverse effects of voids on FDM 3D printing fabricated continuous carbon fiber (cCF) reinforced polymer composite laminates. The PA6/cCF composites had a typical fiber volume fraction of 35%, with fibers uniformly distributed. However, void content as high as 12% was observed in the composites. Further investigation into the effects of voids on the failure mechanism revealed that the associated poor fiber/matrix interfaces were among the main causes of reduced mechanical performance. As a benchmark, the FDM 3D printed PA6/cCF composites with

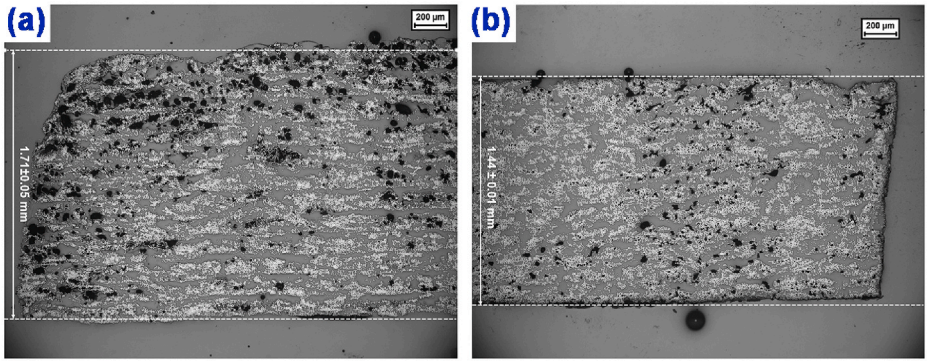

Fig. 14. Micrographs showing typical cross-sections of FDM 3D printed PA6/cCF composites: (a) without and (b) with compression moulding. Reprinted with permission from Ref. [42].

the same configurations were further processed by compression moulding (CM) with thickness controlled to achieve the minimum void content (Fig. 14) so that the impact of such defects could be thoroughly revealed through comparative studies. The results indicated that the presence of voids within the printed PA6/cCF have substantial negative impacts on mechanical performance, as the transverse tensile strength, flexural strength, and interlaminar fracture toughness increased by 78%, 93%, and 90% respectively with the decrease in void content to 6% by CM. By revealing the substantial adverse effects of the microscopic voids in FDM 3D printed composites, this study articulated the critical importance of developing in-process techniques during 3D printing to minimize the formation of voids and decrease the void content within the continuous fiber reinforced polymer composites, for the sake of expanding practical applications of 3D printed continuous fiber reinforced polymer composites.

5. Conclusions and outlook

Recent achievements in the FDM 3D printing of polyamide-base composites and its applications are reviewed in the present work. This burgeoning field has been undergoing rapid development over the past several years, and would open up vast opportunities in practical applications. Special focus is paid on the principle underlying the design and fabrication of polyamide composites for FDM 3D printing and the properties of the FDM 3D printed parts. Although FDM 3D printing of polyamide-based composites has undergone significant progress in recent years, there is still a lot of limitations of this technology that need to be conquered to make it more widely accepted by industries. The work listed in the article is not final, but a start for the development of polyamide-based composites with high performance and diverse functionality for FDM 3D printing. Looking forward to the future, there are still lots of challenges and also opportunities for the FDM 3D printing of polyamide-base composites aiming at improving the comprehensive properties and performance of the printed products.

(1) **FDM 3D printing of polyamide-based nanocomposites.** Nanomaterials such as carbon nanotubes [43,44], carbon nanofibers [45], graphene [4,14,36,37], silica, montmorillonite [13], and other nanomaterials usually exhibit unique mechanical, electrical, and thermal properties. Consequently, the incorporation of nanomaterials into polyamide for FDM 3D printing could be capable of creating high-performance and multifunctional nanocomposites. Chasing for new reinforcement and suitable compositing method is critical for increasing the versatility of FDM 3D printing technology for polyamide-based nanocomposites. In addition, nanocellulose [46], including cellulose nanocrystals (CNCs), cellulose nanofibers (CNFs), and cellulose fibrils (CFs) has gained popularity in 3D printing because of its rheological properties, hydrophilicity, nontoxicity, and versatile surface chemistry, which has potential for economic large-scale processing. This kind of sustainable nanomaterial reinforced polyamide nanocomposites are also promising to be explored to optimize the material cost and environmental impact.

(2) **Multicomponent FDM 3D printing of polyamide-based composites.** The multicomponent FDM 3D printing is a newly developed FDM 3D printing technology with a multi-material feeding system, which has drawn growing attentions in the field of additive manufacturing [7]. Since the different high-power step motors of the multicomponent FDM 3D printer can be respectively controlled through software, the proportion of different materials inside one sample can be achieved arbitrarily, which helps to achieve macroscopic heterogeneity, such as the gradient functional composites [7]. The new polyamide-based composites suitable for multicomponent FDM 3D printing should be developed to construct composite materials with diverse performance and functionality.

(3) **Theory and simulation for FDM 3D printing of polyamide-based composites.** The theory and simulation can provide valuable information which is difficult to be obtained in the experiments. However, the theoretical investigation on polyamide-based composites and FDM 3D printing is still rare and the mechanism behind the modification of polyamide for FDM 3D printing is also unclear. Therefore, the theory and simulation such as self-consistent field theory, molecular dynamics, dissipative particle dynamics, Brownian dynamics, fluid dynamics, and finite element could be developed for examining the composite and printing behavior of polyamide-based composites to reveal the modification mechanism and principle of polyamide for FDM 3D printing. Moreover, the combining simulation methods at different length scales, incorporating the polymer information at molecular level, the structural information at microscopic level, and FDM 3D printing process at mesoscopic or even macroscopic level should also be expanded in the further.

Declaration of competing interest

The authors declare that they have no known competing financial interests or personal relationships that could have appeared to influence the work reported in this paper.

Acknowledgements

This work was financially supported by the Fundamental Research Funds for the Central Universities (Grant No.: 2232020D-11 and 2232019A3-03) and the National Natural Science Foundation of China (Grant No.: 21674019 and 21875033).

References

[1] C.W. Hull, Apparatus for Production of Three-Dimensional Objects by Stereolithography, Google Patents, 1986.
[2] C. Kousiatza, D. Tzetzis, D. Karalekas, In-situ characterization of 3D printed continuous fiber reinforced composites: a methodological study using fiber Bragg grating sensors, Compos. Sci. Technol. 174 (2019) 134–141.
[3] S.C. Daminabo, S. Goel, S.A. Grammatikos, H.Y. Nezhad, V.K. Thakur, Fused deposition modeling-based additive manufacturing (3D printing): techniques for polymer material systems, Mater. Today Chem. 16 (2020) 100248.
[4] V. Tambrallimath, R. Keshavamurthy, D. Saravanabavan, P.G. Koppad, G.S. P. Kumar, Thermal behavior of PC-ABS based graphene filled polymer nanocomposite synthesized by FDM process, Compos. Commun. 15 (2019) 129–134.
[5] J. Wang, T. Senthil, L. Wu, X. Zhang, Enhancement of lightweight composite parts with robust cellular structures by combining fused deposition modeling and electromagnetic induction heating, Adv. Eng. Mater. 20 (8) (2018) 1800215.
[6] X. Zhang, J. Wang, Controllable interfacial adhesion behaviors of polymer-on-polymer surfaces during fused deposition modeling 3D printing process, Chem. Phys. Lett. 739 (2020) 136959.
[7] J. Wang, S. Mubarak, D. Dhamodharan, N. Divakaran, L. Wu, X. Zhang, Fabrication of thermoplastic functionally gradient composite parts with anisotropic thermal conductive properties based on multicomponent fused deposition modeling 3D printing, Compos. Commun. 19 (2020) 142–146.
[8] Y. Jia, H. He, X. Peng, S. Meng, J. Chen, Y. Geng, Preparation of a new filament based on polyamide-6 for three-dimensional printing, Polym. Eng. Sci. 12 (57) (2017) 1322–1328.
[9] W. Zhong, F. Li, Z. Zhang, L. Song, Z. Li, Short fiber reinforced composites for fused deposition modeling, Mater. Sci. Eng. A 301 (2) (2001) 125–130.
[10] X. Wang, M. Jiang, Z. Zhou, J. Gou, D. Hui, 3D printing of polymer matrix composites: a review and prospective, Compos. B Eng. 110 (2017) 442–458.
[11] X. Peng, H. He, Y. Jia, H. Liu, Y. Geng, B. Huang, C. Luo, Shape memory effect of three-dimensional printed products based on polypropylene/nylon 6 alloy, J. Mater. Sci. 54 (2019) 9235–9246.
[12] A.K. Sood, R. Ohdar, S. Mahapatra, Parametric appraisal of mechanical property of fused deposition modelling processed parts, Mater. Des. 31 (1) (2010) 287–295.
[13] Z. Weng, J. Wang, T. Senthil, L. Wu, Mechanical and thermal properties of ABS/montmorillonite nanocomposites for fused deposition modeling 3D printing, Mater. Des. 102 (2016) 276–283.
[14] V. Tambrallimath, R. Keshavamurthy, D. Saravanabavan, P.G. Koppad, G.S. P. Kumar, Thermal behavior of PC-ABS based graphene filled polymer nanocomposite synthesized by FDM process, Compos. Commun. 15 (2019) 129–134.
[15] Y. Li, J. Zhong, L. Wu, Z. Weng, L. Zheng, S. Peng, X. Zhang, High performance POSS filled nanocomposites prepared via UV-curing based on 3D stereolithography printing, Compos. Appl. Sci. Manuf. 117 (2019) 276–286.
[16] Y. Jia, H. He, Y. Geng, B. Huang, X. Peng, High through-plane thermal conductivity of polymer based product with vertical alignment of graphite flakes achieved via 3D printing, Compos. Sci. Technol. 145 (2017) 55–61.
[17] Y. Geng, H. He, Y. Jia, X. Peng, Y. Li, Enhanced through-plane thermal conductivity of polyamide 6 composites with vertical alignment of boron nitride achieved by fused deposition modeling, Polym. Compos. 40 (9) (2019) 3375–3382.
[18] F. Momeni, S.M.M. Hassani, X. Liu, J. Ni, A review of 4D printing, Mater. Des. 122 (2017) 42–79.
[19] J.J. Wu, L.M. Huang, T. Xie, 4D printing: history and recent progress, Chin. J. Polym. Sci. 36 (2018) 563–575.
[20] I. Farina, N. Singh, F. Colangelo, R. Luciano, G. Bonazzi, F. Fraternali, High-performance nylon-6 sustainable filaments for additive manufacturing, Materials 12 (2019) 3955.
[21] M. Nikzad, S. Masood, I. Sbarski, Thermo-mechanical properties of a highly filled polymeric composites for fused deposition modeling, Mater. Des. 32 (6) (2011) 3448–3456.
[22] K. Boparai, R. Singh, H. Singh, Comparison of tribological behavior for nylon6-Al-Al_2O_3 and ABS parts fabricated by fused deposition modelling: this paper reports a low cost composite material that is more wear-resistant than conventional ABS, Virtual Phys. Prototyp. 10 (2) (2015) 59–66.
[23] D. Isakov, Q. Lei, F. Castles, C. Stevens, C. Grovenor, P. Grant, 3D printed anisotropic dielectric composite with meta-material features, Mater. Des. 93 (2016) 423–430.
[24] C.M. Shemelya, A. Rivera, A.T. Perez, C. Rocha, M. Liang, X. Yu, C. Kief, D. Alexander, J. Stegeman, H. Xin, Mechanical, electromagnetic, and X-ray shielding characterization of a 3D printable tungsten polycarbonate polymer matrix composite for space-based applications, J. Electron. Mater. 44 (8) (2015) 2598–2607.
[25] S. Kumar, A. Czekanski, Development of filaments using selective laser sintering waste powder, J. Clean. Prod. 165 (2017) 1188–1196.
[26] R. Soundararaan, N. Jayasuriya, R.G.G. Vishnu, B.G. Prassad, C. Pradeep, Appraisal of mechanical and tribological properties on PA6-TiO_2 composites through fused deposition modelling, Mater. Today Proc. 18 (2019) 2394–2402.
[27] R. Singh, R. Kumar, I.P.S. Ahuja, Mechanical, thermal and melt flow of aluminum-reinforced PA6/ABS blend feedstock filament for fused deposition modeling, Rapid Prototyp. J. 24 (9) (2018) 1455–1468.
[28] R. Kumar, R. Singh, I.P.S. Ahuja, Investigations of mechanical, thermal and morphological properties of FDM fabricated parts for friction welding applications, Measurement 120 (2018) 11–20.
[29] R. Kumar, R. Singh, I.P.S. Ahuja, Friction stir welding of ABS-15Al sheets by introducing compatible semi-consumable shoulder-less pin of PA6-50Al, Measurement 131 (2019) 461–472.
[30] R. Kumar, R. Singh, I.P.S. Ahuja, K.N. Karn, Processing of melt flow compatible thermoplastic composites for solid state welding applications, Mater. Today Proc. 18 (2019) 3167–3173.
[31] R. Singh, R. Kumar, I.P.S. Ahuja, Friction welding for functional prototypes of PA6 and ABS with Al powder reinforcement, Proc. Natl. Acad. Sci., India Sec. A Phys. Sci. (2020), https://doi.org/10.1007/s40010-020-00659-z.
[32] R. Kumar, R. Singh, I.P.S. Ahuja, A. Amendola, R. Penna, Friction welding for the manufacturing of PA6 and ABS structures reinforced with Fe particles, Compos. B Eng. 132 (2018) 244–257.
[33] T.N.A.T. Rahim, A.M. Abdullah, H.M. Akil, D. Mohanad, Z.A. Rajion, The improvement of mechanical and thermal properties of polyamide 12 3D printed parts by fused deposition modelling, Express Polym. Lett. 11 (12) (2017) 963–982.
[34] A.M. Abdullah, T.N.A.T. Rahim, D. Mohamad, H.M. Akil, Z.A. Rajion, Mechanical and physical properties of highly ZrO_2/β-TCP filled polyamide 12 prepared via fused deposition modelling (FDM) 3D printer for potential craniofacial reconstruction application, Mater. Lett. 189 (2017) 307–309.
[35] A.M. Abdullah, T.N.A.T. Rahim, W.N.F.W. Hamad, D. Mohamad, H.M. Akil, Z. A. Rajion, Mechanical and cytotoxicity properties of hybrid ceramics filled polyamide 12 filament feedstock for craniofacial bone reconstruction via fused deposition modelling, Dent. Mater. 34 (2018) e309–e316.
[36] W. Xi, X. Zhang, M. Jin, D. Huang, Z. Shi, 3-D printing technology research on graphene reinforced nylon composites, China Plast. Ind. 44 (12) (2016) 38–50.
[37] D. Zhu, Y. Ren, G. Liao, S. Jiang, F. Liu, J. Guo, G. Xu, Thermal and mechanical properties of polyamide 12/graphene nanoplatelets nanocomposites and parts fabricated by fused deposition modeling, J. Appl. Polym. Sci. 134 (39) (2017) 45332.
[38] F. Li, J. Sun, H. Xie, K. Yang, X. Zhao, Thermal deformation of PA66/carbon powder composite made with fused deposition modeling, Materials 13 (2020) 519.
[39] G. Liao, Z. Li, Y. Cheng, D. Xu, D. Zhu, S. Jiang, J. Guo, X. Chen, G. Xu, Y. Zhu, Properties of oriented carbon fiber/polyamide 12 composite parts fabricated by fused deposition modeling, Mater. Des. 139 (2018) 283–292.
[40] C. Badini, E. Padovano, R.D. Camillis, V.G. Lambertini, M. Pietroluongo, Preferred orientation of chopped fibers in polymer-based composites processed by selective laser sintering and fused deposition modeling: effects on mechanical properties, J. Appl. Polym. Sci. 137 (38) (2020), 49152, https://doi.org/10.1002/app.49152.
[41] C. Kousiatza, D. Tzetzis, Karalekas, In-situ characterization of 3D printed continuous fiber reinforced composites: a methodological study using fiber Bragg grating sensors, Compos. Sci. Technol. 174 (2019) 134–141.
[42] Q. He, H. Wang, K. Fu, L. Ye, 3D printed continuous CF/PA6 composites: effect of microscopic voids on mechanical performance, Compos. Sci. Technol. 191 (2020) 108077.
[43] H. Liu, B. Xu, X. Yang, Z. Li, Z. Mo, Y. Yao, S. Lin, Ultraviolet and infrared two-wavelength modulated self-healing materials based on azobenzene-functionalized carbon nanotubes, Compos. Commun. 19 (2020) 233–238.
[44] W. Li, C. Xu, X. Ren, Y. Xue, J. Zhao, Q. Li, X. Zhang, Anti-fatigue and multifunctional core-spun yarns based on carbon nanotube springs, Compos. Commun. 19 (2020) 127–133.
[45] W. Weng, R. Kurihara, J. Wang, S. Shiratori, Electrospun carbon nanofiber-based composites for lithium-ion batteries: structure optimization towards high performance, Compos. Commun. 15 (2019) 135–148.
[46] M.I. Voronova, O.V. Surov, N.V. Rubleva, N.E. Kochkina, A.V. Afineevskii, A. G. Zakharov, Nanocrystalline cellulose composites with polyvinylpyrrolidone: self-assembly and dispersibility in water, Compos. Commun. 15 (2019) 108–112.